

**MONTE CARLO SIMULATION AND  
EXPERIMENTAL VALIDATION OF PLASTIC  
SCINTILLATOR PERFORMANCE FOR  
RADIATION DETECTION**

**GUNTUR EKO PUTRO**

**UNIVERSITI SAINS MALAYSIA**

**2025**

**MONTE CARLO SIMULATION AND  
EXPERIMENTAL VALIDATION OF PLASTIC  
SCINTILLATOR PERFORMANCE FOR  
RADIATION DETECTION**

by

**GUNTUR EKO PUTRO**

**Thesis submitted in fulfillment of the requirements  
for the Degree of  
Master of Science**

**February 2025**

## ACKNOWLEDGEMENT

All the praises and thanks are to ALLAH SWT, the Lord of mankind and all that exists. I extend my gratitude to my supervisor, Dr. Muhammad Rabie bin Omar, for his unwavering support and guidance throughout the entirety of my research journey. I am appreciative of the National Research and Innovation Agency for their generous support, which has enabled me to pursue this research endeavor. I am also indebted to my colleagues for their invaluable contributions and constructive feedback, which have greatly enhanced the quality of this thesis.

Finally, I am grateful to my family for their unwavering encouragement, love, and understanding throughout my academic pursuits. Their unwavering support and belief in my abilities have been a constant source of motivation, inspiring me to strive for excellence and persevere in the face of challenges. To all those mentioned above and to countless others who have supported me along this journey, I offer my sincerest thanks. Your contributions have been indispensable, and I am deeply grateful for the opportunity to have collaborated with such exceptional individuals.

## TABLE OF CONTENTS

<b>ACKNOWLEDGEMENT</b> .....	<b>ii</b>
<b>TABLE OF CONTENTS</b> .....	<b>iii</b>
<b>LIST OF TABLES</b> .....	<b>v</b>
<b>LIST OF FIGURES</b> .....	<b>vi</b>
<b>LIST OF SYMBOLS</b> .....	<b>viii</b>
<b>LIST OF ABBREVIATIONS</b> .....	<b>x</b>
<b>LIST OF APPENDICES</b> .....	<b>xiii</b>
<b>ABSTRAK</b> .....	<b>xiv</b>
<b>ABSTRACT</b> .....	<b>xvi</b>
<b>CHAPTER 1 INTRODUCTION</b> .....	<b>1</b>
1.1 Background .....	1
1.2 Problem Statement .....	3
1.3 Objectives.....	5
1.4 Scope and Limitations .....	6
1.5 Thesis Outline .....	6
<b>CHAPTER 2 THEORY AND LITERATURE REVIEW</b> .....	<b>8</b>
2.1 Scintillation and Photomultiplier Tube (PMT) .....	8
2.2 Monte Carlo Method .....	11
2.3 Energy Resolution and FWHM.....	12
2.4 Detector Efficiency .....	13
2.4.1 Detector Properties Effect.....	17
2.4.2 Incident Radiation Characteristics .....	17
2.4.3 Electronic Devices .....	18
2.5 Pulse-Height Distribution.....	18
2.6 Gaussian Energy Broadening (GEB) .....	21

<b>CHAPTER 3</b>	<b>METHODOLOGY.....</b>	<b>25</b>
3.1	Experimental Work .....	25
3.2	Monte Carlo Simulation .....	30
3.2.1	MCNP Input File.....	32
3.2.2	Cell cards.....	33
3.2.3	Surface cards .....	34
3.2.4	Data cards.....	36
3.2.4(a)	Mode Cards .....	37
3.2.4(b)	Surface And Cell Attribute Cards .....	38
3.2.4(c)	Source Definition Cards .....	40
3.2.4(d)	Tally Definition Cards.....	42
3.2.4(e)	Materials Definition Cards .....	43
3.2.5	Scenario Termination .....	45
3.2.6	Variance Reduction (Cell Importance) .....	46
3.3	Energy Resolution and Efficiency Calculation .....	48
<b>CHAPTER 4</b>	<b>RESULTS AND DISCUSSIONS .....</b>	<b>51</b>
4.1	Comparative Study on Pulse Height Spectrum .....	51
4.2	Study on GEB Effect on Simulation Results .....	56
4.3	Scintillator Efficiency .....	58
4.4	Energy Resolution and FWHM Profile .....	63
4.5	Summary and Limitations .....	66
<b>CHAPTER 5</b>	<b>CONCLUSION AND RECOMMENDATIONS .....</b>	<b>68</b>
5.1	Conclusion.....	68
5.2	Recommendations and Future Works .....	69
<b>REFERENCES.....</b>		<b>70</b>
<b>APPENDICES</b>		
<b>LIST OF PUBLICATIONS</b>		

## LIST OF TABLES

	<b>Page</b>
Table 3.1 Photon sources for spectrum measurements (Lee et al., 2017).....	25
Table 3.2 Surface Cards in MCNP Input (Werner, 2017).....	35
Table 3.3 List of MCNP Particles (Werner, 2017) .....	37
Table 4.1 Comparison of simulated and experimental results for some variables....	59

## LIST OF FIGURES

	Page
Figure 2.1 Scintillation counting diagram and spectrum of pulse height (Hamamatsu Photonics K.K., 2017).....	9
Figure 2.2 PMT and scintillator configuration in gamma detection (Hamamatsu Photonics K.K., 2017).....	10
Figure 2.3 Photon counting head diagram (Hamamatsu Photonics K.K., 2017)....	11
Figure 2.4 FWHM determination technique from pulse height distribution. ....	13
Figure 2.5 Schematic of particle trajectories upon interaction with the detector (Knoll, 2010) .....	14
Figure 2.6 Configuration of the scenario for photon detection (Knoll, 2010).....	15
Figure 2.7 The experimental setting utilised to investigate energy straggling (Knoll, 2010) .....	22
Figure 2.8 Particle straggling around A. 3.2 mg/cm <sup>2</sup> and B. 32 mg/cm <sup>2</sup> silver films (Tsoulfanidis & Landsberger, 2015).....	23
Figure 3.1 Illustration of the experimental configuration.....	27
Figure 3.2 Assembly of the measurement device.....	29
Figure 3.3 Prepared detector for spectrum measurements.....	30
Figure 3.4 Plastic detector geometry in the current study .....	31
Figure 3.5 The Monte Carlo code flowchart in connection to experimental work. ....	50
Figure 4.1 Pulse height profile for simulation and experimental results: A. <sup>137</sup> Cs; B. <sup>60</sup> Co.....	53
Figure 4.2 Cross validation curve for simulation and experimental results: A. <sup>137</sup> Cs; B. <sup>60</sup> Co.....	55
Figure 4.3 Pulse height spectrum obtained from simulation with and without GEB treatment.....	57
Figure 4.4 Efficiency curve of plastic detector based on experimental and simulation results.....	61
Figure 4.5 Comparison of detector efficiency (%) of NaI(Tl) detector based on experimental (Salgado et al) and simulation (current study) results. ....	62

Figure 4.6 Curve profile comparison of A. FWHM; B. Energy resolution..... 64

## LIST OF SYMBOLS

$Z$	Atomic Number
$R$	Detector Resolution
$E_0$	Peak Level of Energy
$\varepsilon$	Detector Efficiency
$N_c$	The Number of Particles Detected
$N_e$	The Number of Particles Impacted
$r$	Net Count in Counts per Second (Cps)
$\Omega$	Solid Angle
$F$	Total Impact of All Adjustment Variables
$d$	Distance
$L$	Detector Length
$R$	Radius
$\theta$	Radiation Angle
$\mu$	Mass Attenuation Coefficient
$T$	Total Energy Deposition
$K$	Number of Entries for Specific Cell
$L$	Number of Departures for Specific Cell
$E_i$	The Tally Energy of $i^{th}$ Particle Entering Specific Cell
$D_j$	The Tally Energy of $j^{th}$ Particle Departing Specific Cell
$\Delta x$	Trajectory Path
$Z_{1,2}$	The Charge of The Incoming Particle
$D_x$	Thickness of Material
$N$	Number of Atoms per cubic meter

$r_o$	Particle Radius
$\Gamma_d$	Energy Straggling Width
$\alpha, \beta, \delta$	Constitute Coefficients
$S$	Generated Photons per Second

## LIST OF ABBREVIATIONS

$^{137}\text{Cs}$	Cesium-137 Isotope
$^{60}\text{Co}$	Cobalt-60 Isotope
AAA	Mass Number
C	Cosine Bin Cards
cc	Centimeter Cubic
CEL	Cell Card
CNNs	Convolutional Neural Networks
cps	Counts/Sec
DA	Delay Amplifier
DE	Dose Energy
DF	Dosage Function
DIR	Directory Function
DS	Dependent Source Distribution
E	Energy Bin Cards
e	Electron
EXT	Exponential Transform Card
FLUKA	Fluktuierende Kaskade
FM	Tally Multiplier
FWHM	Full Width at Half Maximum
Geant4	GEometry ANd Tracking 4
GEB	Gaussian Energy Broadening
H	Proton
<i>imp</i> , IMP	Importance

INP	Input File
KCODE	Criticality Definition Card
keV	Kilo Electron Volt (Energy Unit)
M <sub>1,2</sub>	Material Card
MC	Monte Carlo
MCA	Multi Channel Analyzer
MCNP	Monte Carlo N-Particle
MeV	Mega Electron Volt (Energy Unit)
M <sub>m</sub>	Material Card
mV	Milli Volts
N	Neutron
NaI(Tl)	Sodium Iodide Detector
npp	Number of Histories
NPS	History Threshold Card
ns	Nano Second
P	Photon ( $\gamma$ )
PHA	Pulse Height Analyzer
PHYS	Physics Card
pl	Particle List
PMT	Photomultiplier Tube
POS	Position Card
RAD	Radian Function
RD	Relative Difference
SD	Segment Divisor
SDEF	Source Definition Card

SI	Source Information
SSR	Surface Source Read
SUR	Surface Function
T	Time Bin Cards
V, $\nu_m$	Muon Neutrino
WW	Weight Window
ZAID	Nuclide Identification Number
ZZZ	Atomic Number

## **LIST OF APPENDICES**

Appendix A    Card File for Simulation Model

# **SIMULASI MONTE CARLO DAN PENENTUSAHAN EKSPERIMEN PRESTASI PENERDIP PLASTIK UNTUK PENGESANAN RADIASI**

## **ABSTRAK**

Sintilator plastik telah digunakan secara meluas untuk mengesan sinaran dalam pelbagai jenis aplikasi. Dalam pengukuran sebenar, prestasi pengesanan yang lemah boleh menyebabkan kecekapan pengesanan yang rendah, meningkatkan risiko terlepas pandang sinaran berbahaya dan menyebabkan kesilapan dalam diagnosis atau memantau tahap pendedahan. Untuk mengurangkan cabaran ini, usaha diperlukan untuk meningkatkan kecekapan pengesanan, memerlukan pembangunan model simulasi yang teguh dan disahkan untuk mempercepatkan kerja ini. Kaedah Monte Carlo digunakan dalam kerja ini membangunkan model pengesan dan menentukan parameter pengesan terdedah kepada sinaran dengan tenaga dari 100 hingga 1300 keV. Prestasi pengesan plastik telah dimodelkan menggunakan MCNP, yang termasuk pelarasan Gaussian Energy Broadening (GEB) untuk mendapatkan respons. Hasil simulasi kemudiannya dibandingkan dengan data eksperimen sebenar untuk menentukan ketepatan. Penyelidikan ini bertujuan untuk mengesahkan hasil simulasi menggunakan data eksperimen. Kajian ini membincangkan pemahaman tentang kekangan dan kemungkinan kod pemodelan, menghasilkan penyelidikan yang lebih cekap menggunakan model simulasi yang disahkan. Keluk pengedaran telah ditentukan menggunakan kedua-dua simulasi dan kerja eksperimen, dan penilaian perbandingan hasil mencadangkan tahap penjajaran yang sesuai dan membentangkan kebolehpercayaan kaedah Monte Carlo dalam menganalisis prestasi pengesan. Selain itu, kajian ini juga bertujuan untuk mengkaji kesan pelarasan Gaussian Energy

Broadening (GEB) terhadap hasil simulasi. Siasatan ke atas pembetulan Gaussian Energy Broadening (GEB) melalui analisis perbandingan menggunakan sumber  $^{137}\text{Cs}$  dan  $^{60}\text{Co}$  mencadangkan bahawa simulasi tanpa GEB mempamerkan nilai yang lebih besar untuk puncak Compton berbanding dengan yang mempunyai GEB. Nilai yang lebih tinggi adalah disebabkan oleh kegagalan untuk mengambil kira isu yang ditemui dalam aplikasi sebenar. Dengan menggabungkan GEB, simulasi kelihatan lebih dipercayai kerana ia menggabungkan kesan realistik ini.

**MONTE CARLO SIMULATION AND EXPERIMENTAL VALIDATION OF  
PLASTIC SCINTILLATOR PERFORMANCE FOR RADIATION  
DETECTION**

**ABSTRACT**

Plastic scintillators have been extensively utilised for detecting radiation in many different kinds of applications. In actual measurement, poor detection performance can lead to low detection efficiency, increasing the risk of overlooking harmful radiation and causing mistakes in diagnosis or monitoring exposure levels. To mitigate these challenges, efforts are required to enhance the detection efficiency, necessitating the development of a robust and validated simulation model to expedite this work. The Monte Carlo method is used in this work to develop detector model and determine parameter of a detector exposed to radiation sources with energies from 100 to 1300 keV. The plastic detector performance was modeled using MCNP, which included Gaussian Energy Broadening (GEB) adjustment for obtaining responses. The simulated outcomes were then compared to actual experimental data to determine accuracy. This research is aimed at verifying simulation outcomes using experimental data. The study discussed understanding the constraints and possibilities of modelling codes, resulting in more efficient research using verified simulation models. The distribution curve has been determined using both simulation and experimental work, and a comparative assessment of outcomes suggested an appropriate level of alignment and presented the Monte Carlo method's reliability in analysing detector performance. In addition, this study also aims to study the effect of Gaussian Energy Broadening (GEB) adjustment on simulation results. The investigation on the Gaussian Energy

Broadening (GEB) correction through comparative analysis utilising  $^{137}\text{Cs}$  and  $^{60}\text{Co}$  sources suggested that simulations without GEB exhibited greater values for the Compton peak in comparison to those with GEB. The higher values are due to a failure to account for issues found in the actual application. By incorporating GEB, simulations appear more reliable since they incorporate these realistic impacts.

# CHAPTER 1

## INTRODUCTION

### 1.1 Background

Significant continuous studies and advancements in inorganic detection system innovation have contributed in the appearance of compounds including  $\text{LaBr}_3(\text{Ce})$ , that feature good light emission properties and rapid decay (Saizu & Cata-Danil, 2011). Nevertheless, it is crucial to recognise that inorganic detection systems remain subject to constraints, including hygroscopic effects, that necessitate careful care and protection using a non-reactive substance and container (Knoll, 2010), in addition to its comparably more expensive production expenses.

Plastic scintillators, on the other hand, deliver substantial advantages through their relatively low density, strong light generation, and quick identification reaction, which is characterised by a decay interval of 4 ns (Kang et al., 2021). These detectors are inexpensive and could be effortlessly moulded to substantial quantities utilising moulding, extrusion, or casting. In order to overcome constraints related to Compton scattering, the present investigation has focused on the combined use of more complex Z molecules, notably bismuth triphenyl and tripivalate bismuth (Cherepy et al., 2018), that exhibit prospects in enhancing peak recognition.

The Monte Carlo N-Particle (MCNP) code has been utilised in this study to develop detector model and determine parameter of a detector for future optimization. The code utilised throughout the present research enhances our capacities to evaluate the response capabilities of this specific detector. MCNP algorithm is capable of accurately calculating the deposited energy of any substance it currently studies. Furthermore, because the photomultiplier tube (PMT) includes collisions between

particles within the actual size, the computer simulation outcomes offer a good, thorough modelling of the scintillator's performance (Salgado et al., 2012). The association between calculation and observation highlights the simulation approach's reliability and precision.

The MCNP algorithm incorporates the robust Monte Carlo method capable of recreating an extensive number of particle inputs. Alternative to modelling the Boltzmann transport equation, this algorithm calculates it by modelling unique particle directions and extracting certain characteristics corresponding to their common properties (Kovaltchouk & Machrafi, 2011). This illustrates the sequential modelling of probabilistic events involving particle interaction with substances, employing statistically determined distributions of chances and pseudo-random outcome extraction. This extensive technique analyses objects throughout their point of origin to their contacts inside a substance until they accomplish an assigned energy termination while keeping in consideration variables including evasion, physical restriction and absorption (Zieb et al., 2018).

Probability distributions are randomly selected from MCNP transport records. These distributions are then used to determine the results at each stage of the object's direction. The essential quantities are computed, together with estimations regarding the analytical correctness of the results. This code is appropriate for simulating photon collisions such as the Bremsstrahlung influence, fluorescence, Thompson and Compton scenarios, and pair creation. The code program additionally has the ability to anticipate discrete element directions while simulating stochastic particle-material interactions (Werner, 2017).

Even though the improvements made in computational procedures, it remains pertinent to emphasise that the number of radiation escaping out of a photomultiplier

release might differ substantially. This unforeseen conduct is an essential element of the scintillator's outstanding accuracy and selectivity. As a consequence, it is critical to take into consideration such variance in energy output during modelling, and evidence from experiments holds a vital part in accomplishing this (Mouhti et al., 2018). The combination of robust models and experimental evidence provides a more thorough understanding of the scintillator's functioning and assures the precision of how it responds while implemented in actual scenarios.

The purpose of this research is to investigate the differences between simulation and practical situations by verifying the simulation outcomes with data obtained from experiments. This work shows that Monte Carlo simulations adequately describe the real experiments. The research will highlight on the drawbacks and advantages of computer programmes and to which the outcomes replicate actual lab tests. The combination of Monte Carlo programmes with verification by experiment may conclude in highly efficient studies due to verified mathematical models for simulation might eliminate the requirement for lengthy and high-priced trials. Furthermore, this study provides valuable insights by determining reliable parameters that can serve as a foundation for future research aimed at further improvements and optimization. Additionally, the outcomes aim to emphasise the significance of Gaussian Energy Broadening (GEB) treatment and highlight the ways that the GEB adjustment might affect the outcomes of simulations, hence closing the disparity between mathematical forecasts and actual evidence.

## **1.2 Problem Statement**

The radiation detection techniques depend significantly on detector performance. Proper analysis becomes challenging without robust detectors that offer

adequate accuracy (El-Khatib et al., 2012, 2013). When analyzing information from multiple applications, efficiency is crucial (Conway, 2010). Numerous obstacles are encountered in real operations due to the limited reliability of detectors. This can complicate radiation identification, leading to critical or potentially deadly exposure going unnoticed and restricting the detector's ability to monitor or measure radiation levels. If this issue continues to exist and a significant amount of emitted radiation goes unreported, the level of radiation received by humans and the environment might rise. Furthermore, since plastic scintillators are used for both medical and commercial screening and radioactivity inspection, inadequate efficiency could result in mistakes in diagnosing and detecting harmful radiation doses. This may have a detrimental influence on medical treatment decisions or actions performed based on misleading data.

To resolve these challenges, a study needs to be conducted to guarantee and enhance detector efficiency. Considering the substantial costs of scientific studies, a study using simulations is necessary to accelerate the process while lowering the cost of expensive tests. Additionally, since experimental procedures could result in elevated doses of ionizing radiation, computer simulation studies have become significantly more vital in lowering the harmful effects of radiation. This demonstrates the rising relevance of simulation studies, not just as an affordable alternative, but also as the primary strategy for reducing potential radiation exposure during laboratory experiments. Consequently, a reliable MCNP simulation framework needs to be developed and validated which will be used for future optimization.

Since the physical phenomena occurring in radiation detection are influenced by the Gaussian Broadening effect, it is also crucial to discuss this effect in both simulations and experimental procedures. The Gaussian Broadening effect can impact

the accuracy and resolution of radiation detectors, as it represents the spread in energy measurements due to various intrinsic and extrinsic factors.

In simulation studies, accurately modeling the Gaussian Broadening effect is essential to ensure that the simulated detector responses closely match actual conditions. This involves incorporating statistical methods and algorithms that can replicate the broadening effect seen in experimental data. By doing so, simulations can provide more reliable predictions about detector performance and help in fine-tuning detector designs before actual physical testing.

### **1.3 Objectives**

The primary objectives including specific objectives which are related to the successful completion of the primary goal are outlined below:

1. Development and validation of the MCNP code model.
  - a. To develop and code a detector model in MCNP that accurately simulates experimental conditions and collects simulation data.
  - b. To validate and verify the reliability of the developed simulation model by comparing the simulated data with experimental data.
2. Investigation of the impact of GEB parameters on simulation outcomes.
  - a. To determine and input the appropriate GEB parameters from experimental data into the MCNP simulation.
  - b. To analyze the effects of GEB adjustments by conducting comparative studies on simulation results with and without the inclusion of GEB parameters.

## 1.4 Scope and Limitations

In this study, we developed the MCNP code for all Monte Carlo (MC) detector response simulations. These simulations include three models: the polystyrene detector model for pulse height spectrum calculation, Gaussian Energy Broadening (GEB)-based MCNP models, and a specific detector model to be compared with a prior investigation. All simulations and calculations in this study were conducted on a Windows environment laptop equipped with an Intel Core i7-7700HQ CPU, utilizing 8 parallel processes. This computational capacity allowed for simulations of up to 1 million histories per MC cycle with an appropriate simulation duration. It is important to acknowledge that the results of performance assessment may differ based on the choice of programming languages, operating systems, and computational hardware used in the study.

## 1.5 Thesis Outline

This thesis is organised into five chapters: introduction, theory and literature review, methodology, results and discussions, and conclusion. **Chapter One** presents the research background, the problem statement, the research objectives, and the thesis outline. **Chapter two** discusses the relevant theory for this research, specifically the radiation detection key parameters and the Monte Carlo pulse height calculation. **Chapter three** covers the framework of simulation model formulation and experimental trials for pulse height spectrum of polystyrene detector, and Gaussian Energy broadening (GEB) based MCNP models. **Chapter four** studies the outcomes of three distinct frameworks: the pulse height spectrum for a polystyrene detector, Gaussian Energy Broadening (GEB)-based MCNP models, and a comparison of detector performance between the current study and a prior investigation. Finally,

**chapter five** summarizes the findings that address the research problem and suggests perspectives to advance the research field.

## CHAPTER 2

### THEORY AND LITERATURE REVIEW

This chapter presents the theory supporting this research. The theory regarding the processes of scintillation and photomultiplier will be discussed, along with the fundamental concepts of Monte Carlo simulation and several key parameters in radiation detection such as energy resolution, FWHM, detector efficiency, pulse height spectrum, and Gaussian Energy Distribution.

#### 2.1 Scintillation and Photomultiplier Tube (PMT)

Scintillation is caused by the event where particle radiation passes through a scintillator, which is defined as a fluorescent having a quick decay period. In the scenario of radiation from gamma rays, the scintillation results from the bound electrons excitation via interactions with free electrons within the scintillator. The free electrons come into existence by three main correspondences: pair generation, Compton effect and photoelectric. The possibility of the phenomena occurring is affected by several parameters, including the scintillator type and the incoming particle energy. Different scintillator materials have varied propensities for each contact process, resulting in unique scintillation properties. Furthermore, the energy spectrum of the incoming gamma rays determines the relative incidence of these interactions, with higher-energy gamma rays supporting some interaction types over others.

Among the three interactions previously mentioned, the scintillation resulting from the photoelectric effect has a notable feature: the amount it produces is precisely proportional to the energy of the incoming gamma ray. This correlation is due to the fact that the photoelectric process transfers all of the gamma-ray energy to the orbital

electrons in the scintillator material. As a result, the photomultiplier tube (PMT) generates an electrical charge proportionate to the quantity of scintillation, providing that the pulse height output obtained from the PMT corresponds to the energy of the incident radiation (Knoll, 2010).

As a result, integrating a scintillator with a photomultiplier tube within a scintillation counter provides an accurate means of evaluating the energy spectrum and dosage. This is accomplished by measuring the pulse height and counting rate results. However, extra procedures are necessary to conduct a more advanced examination of radiation energy. This includes employing an integrated preamplifier to convert PMT current output to voltage. The resulting voltage signal is then sent to a Pulse Height Analyzer (PHA), which allows for the investigation of pulse height distributions. Figure 2.1 depicts a standard diagram of scintillation, which illustrates this procedure. This diagram depicts the steps required to convert scintillation events into recognisable electrical signals for further examination (Hamamatsu Photonics K.K., 2017).

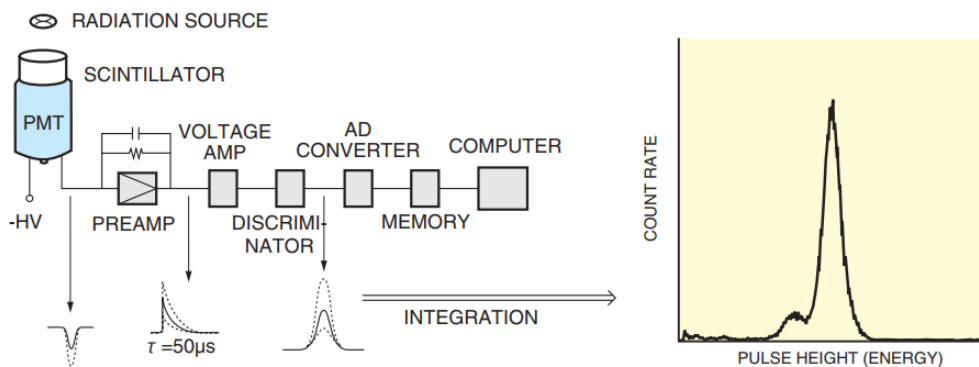


Figure 2.1 Scintillation counting diagram and spectrum of pulse height (Hamamatsu Photonics K.K., 2017)

In the configuration depicted in Figure 2.2, a scintillator is closely attached to a photomultiplier tube using the utilization of a coupling agent. The primary purpose of using this coupling agent is to fill any air gaps, reducing optical losses in the space between the faceplate of the photocathode and the scintillator. Silicone oil, which is well-known for having a refractive index that is almost identical to that of the glass faceplate, is a preferred coupling agent in such setups.

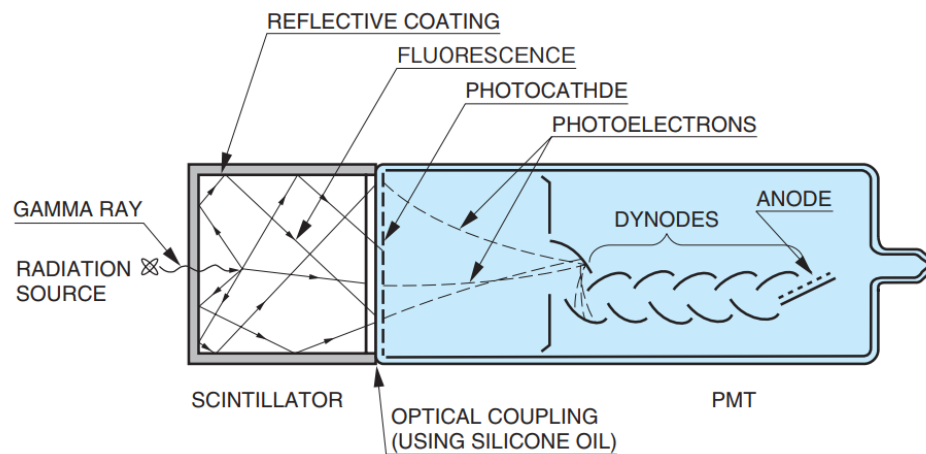


Figure 2.2 PMT and scintillator configuration in gamma detection (Hamamatsu Photonics K.K., 2017)

Photomultiplier modules typically consist of a PMT unit, a power supply that provides high voltage, and a voltage divider that supplies voltage through each electrode. Beyond this essential configuration, PMT modules may include extra features to increase their adaptability and value in a variety of applications. These supplemental elements frequently include an amplifier circuit to convert current into voltage, a particle-counting circuit, a cooling device and a computer interface. By including these auxiliary components, PMT modules improve functionality and convenience of use by reducing the need for complex high voltage.

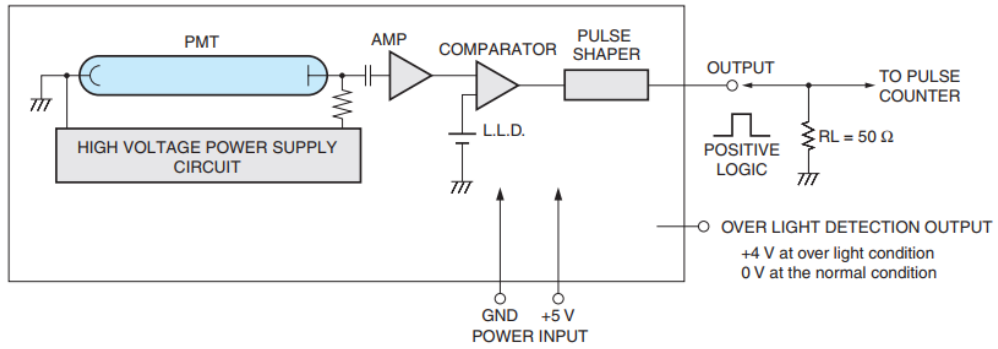


Figure 2.3 Photon counting head diagram (Hamamatsu Photonics K.K., 2017)

The pulses from the PMT are amplified in the head amplifier during the photon counting operation as depicted in Figure 2.3. These amplified pulses are subjected to a threshold level, which allows only pulses that are above the specified threshold to pass the pulse shaper before eventual pulse output. These devices are pre-adjusted to ensure that the photomultiplier tube receives a high voltage that falls under the plateau range, allowing for consistent photon detection results. The operating requirements for photon counting heads require only a low voltage input from an external power supply to maintain performance.

## 2.2 Monte Carlo Method

The Monte Carlo (MC) has emerged as a commonly utilised stochastic algorithm-based computation solution which has been utilised for numerous kinds of nuclear fields. It covers major challenges related to radiation protection, nuclear plant design, radiation safeguarding modelling, and detection system modelling, and contributes to the management of potentially harmful dosages of radiation. The stochastic element becomes apparent by its reliance on statistically determined

samples regarding probability models across space, which allows for the modelling of particle movement in a certain setting (Kilby et al., 2019).

Monte Carlo has become a reliable method used for assessing detector responses, and advances in information technology have made it an effective and most probably more advantageous alternative to older methodologies. Multiple research projects employing this method for estimating detector performance yielded encouraging findings. LaBr<sub>3</sub> and NaI detectors constitute two significant detectors which have already been investigated using this technology (Casanovas et al., 2012; Mouhti et al., 2018; Salgado et al., 2012). In addition, the Monte Carlo procedure has emerged as an increasingly important computational modelling method for the nuclear field in situations where actual measurements tend to be difficult or complex, such as when obtaining data for creating and developing machine learning algorithms to aid in many different kinds of nuclear fields.

Various benefits of using the Monte Carlo method involve the ability to set up tests in laboratories requiring no utilisation of any radioactive materials and delivering reliable computing outcomes. To investigate the motion of particles in a specific computer simulation environment, the technique incorporates stochastics, which are based on gathered information from suitable concentration probabilities. An individual photon's randomised "history" is typically determined by its entire existence from the starting point to its completion (which incorporates absorption followed by discharge away the threshold) (Asano et al., 2022).

### **2.3 Energy Resolution and FWHM**

The resolution of the detector measures the capability of the detector to identify photons having nearly identical energy. The natural resolution of a detector typically

surpasses the achievable resolution. The detector resolution ( $R$ ) can be described as the ratio of FWHM to the maximum level of energy ( $E_0$ ) as follows:

$$R = \frac{FWHM}{E_0} \quad (2.1)$$

The FWHM can be obtained by determining the peak length at the 50% of the highest value of the profile peak. It can be described as the length separating two places where the peak level equals fifty per cent of the highest peak, as shown in Figure 2.4. This methodology measures how much separated the peaks in an obtained spectrum are. FWHM may be used in radiation detection systems to evaluate the detector's efficiency to recognise and measure the energy of various particles that pass through the detector (Tsoulfanidis & Landsberger, 2015).

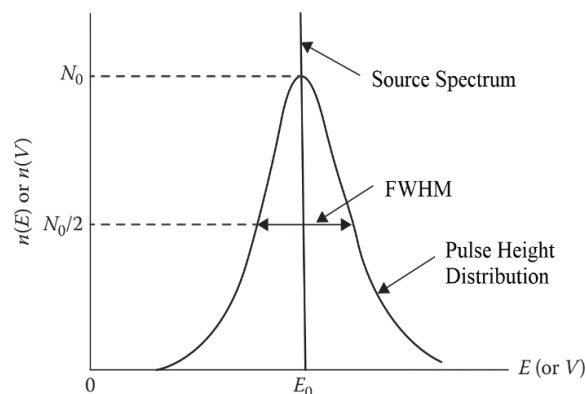


Figure 2.4 FWHM determination technique from pulse height distribution.

## 2.4 Detector Efficiency

The certainty of particle detection upon entry into a detector stands unpredictable, determined by a variety of parameters such as particle type, energy, and detector properties. As shown in Figure 2.5, a particle may pass through the detector without interacting, especially when considering the dimensions and type of the

detector. Additionally, the particle may produce a signal that is too weak to be detected by the existing electronic equipment, as shown by particle 3, or it might encounter an obstacle in the detector window, preventing it from entering the detector, as shown by particle 4. In this setting, particle 2 appears to have a greater possibility of being identified.

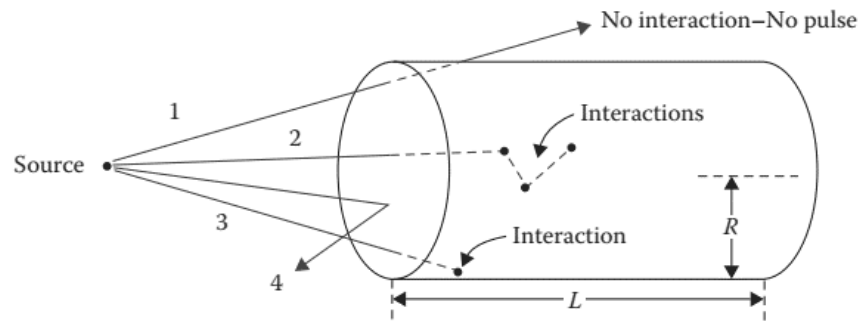


Figure 2.5 Schematic of particle trajectories upon interaction with the detector (Knoll, 2010)

The efficiency parameter,  $\varepsilon$ , calculated by Eq. (2.2), quantifies the proportion of particles effectively detected.

$$\varepsilon = \frac{N_c}{N_e} \quad (2.2)$$

Where  $N_c$  denotes the number of particles detected for each time frame and  $N_e$  represents the number of particles impacted over the detector for each time frame.

The determination of a detector's efficiency may be achieved through both experimentally or theoretically. While there are several techniques for assessing efficiency, one of the easiest and most accurate alternatives is to utilise a standardised source with known properties. Figure 2.5 depicts a scenario in which the source works as a monoenergetic isotropic emitter, generating  $S$  photons every second. In this context, the net count is indicated as  $r$  counts/sec (cps), the efficiency is denoted as  $\varepsilon$

and the solid angle is represented by  $\Omega$ . The equation defining the efficiency is provided by:

$$\varepsilon(E) = \frac{r}{\Omega F(E) S} \quad (2.3)$$

$F$  indicates the total impact of all adjustment variables, represented as  $f_a$  and so on, that may be required to apply to the outcomes. It is important to note that both the adjustment variables and the efficiency are determined by the particle energy under consideration. While precise measurements are often based on empirically measured efficiencies, theoretical estimates of efficiency remain useful for illustrating important aspects. In the following discussion, a scenario of efficiency estimation for a photon detector will be described providing an understanding of the theoretical that supports efficiency evaluations.

In the configuration of the scenario outlined, a single-point monoenergetic isotropic source is positioned at a distance ( $d$ ) from a cylindrical form detector of length ( $L$ ) and radius ( $R$ ), as illustrated in Figure 2.6.

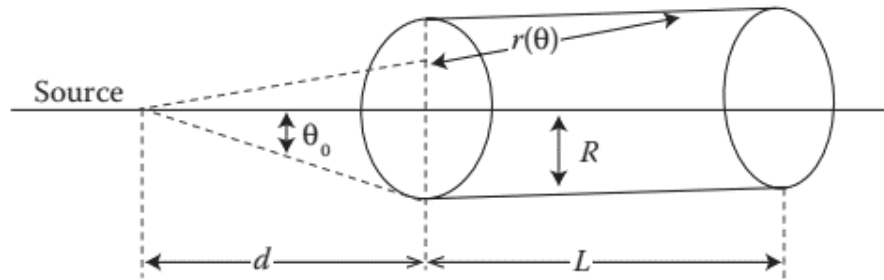


Figure 2.6 Configuration of the scenario for photon detection (Knoll, 2010)

The possibility of contact for photons radiated at an angle ( $\theta$ ) relative to the detector axis can be calculated as  $1 - e^{-\mu(E)r(\theta)}$ , whereas the possibility of emission

occurring across  $\theta$  to  $(\theta + d\theta)$  can be quantified by  $\frac{1}{2} \sin \theta d\theta$ . The detection efficiency is then determined by Eq. (2.4), assuming that a single contact is sufficient to create an identifiable pulse.

$$\varepsilon(E) = \frac{\int_0^{\theta_0} S\{1 - e^{[-\mu(E)r(\theta)]}\} \cdot \frac{1}{2} \cdot \sin \theta d\theta}{\left(\frac{S}{2}\right) \cdot \int_0^{\theta_0} \sin \theta d\theta} \quad (2.4)$$

Eq. (2.4) demonstrates that the detection efficiency is dependent to not solely on the variables of energy, mass attenuation and length but also upon the distance of the source-detector and the detector radius. As a result, while evaluating the efficiency of a point isotropic particle, it is necessary to include the geometry factor as an intrinsic component of the computation. Eq. (2.4) potentially to lead in an overestimation of efficiency since it is based on the assumption that contact of the incoming photon to the detector would always generate an identifiable pulse. However, this assumption may not always be valid in practice.

A more precise method of evaluating efficiency requires computing the total energy deposition in the detector as an outcome of interactions with the incoming particle. The number of recorded particles may then be determined by calculating the minimal energy threshold necessary to produce a pulse that exceeds the discriminator threshold. In the accomplishment of this purpose, the Monte Carlo technique emerges as a particularly effective instrument. The Monte Carlo approach, which is recognised for its precision, has been widely adopted by researchers for precisely this reason. In actual measurements, a variety of factors impact the detector efficiency ( $\varepsilon$ ) including but not limited to detector properties, incident radiation characteristics, and electronic devices.

### **2.4.1 Detector Properties Effect**

The probability of interaction between incoming radiation and the detector material determines its efficiency. The probability is intrinsically determined by the detector size; a greater detector size is often associated with a higher probability of contact. However, the value of enlarging the detector is limited by two fundamental factors: the resulting increase in background radiation and the practical limits inherent in the construction of large-scale detectors. Notably, semiconductor detectors illustrate this difficulty, as scaling up in scale presents considerable technical challenges.

The possibility of contact per unit distance travelled is directly related to the material density. Under standard temperature and pressure conditions, liquids and solids have densities that are about a thousand times larger than gases. As a result, solid or liquid detectors are naturally more efficient than their gaseous equivalents.

### **2.4.2 Incident Radiation Characteristics**

When charged particles travel through a material, they will unavoidably interact with the nuclei and electrons that constitute its structure. Given the near certainty of these interactions, charged particle detectors generally approach 100% efficiency. This extraordinary efficiency remains steady regardless of the detector size or the density of the material used. Notably, the effectiveness of charged particle detectors is mainly unaffected by particle energy, with the exception of particularly low energy scales, as particles could be blocked by the window.

Neutrons and photons, on the opposite, indicate exponential attenuation as they travel through a material. This attenuation characteristic means there will be a non-zero possibility that the particle will pass through any particular thickness of substance

without interacting. Consequently, neutron or photon detectors are often less than 100 percent efficient, irrespective of their size or particle energy.

### **2.4.3 Electronic Devices**

The efficiency of a counting system is substantially influenced by its electronic components, although indirectly. When a particle contacts with the detector, it generates a signal, and its recording is dependent on the effective registration of that signal. The signal is only considered recorded if it exceeds the discriminator threshold, that is defined by the electronic disturbance inherent in the counting mechanism. As a result, reducing electronic disturbance levels has the potential to increase efficiency.

For instance, assume a system for counting with noise levels that suggest a discriminator threshold of 1 mV. In such a scenario, pulses with only a greater than 1 mV are countable. As a result, particles that generate pulses below this threshold are not recorded. Consider a scenario in which either the preamplifier, amplifier or a pair are replaced using quieter alternatives, decreasing electronic noise levels. As a result, the discriminator threshold may now be adjusted to a lower threshold, such as 0.8 mV. Thus, pulses as low as 0.8 mV may now be detected, allowing for the registration of more particles and increasing the overall efficiency of the counting. When addressing electronics in terms of counting efficiency, it is critical to evaluate the efficiency of the complete system, which includes both the detector and the electronic components.

## **2.5 Pulse-Height Distribution**

The MCNP simulation departs from microscopic realism in numerous aspects of its functioning. Notably, in MCNP, the sampling of the supplementary neutrons and photons generated by a neutron collision happens independently, with no fundamental

connection between the released particles and without regard for energy conservation. This absence of correlation provides a level of stochasticity in the simulation results. Similarly, in the case of electron interactions, changes in the energy loss rate do not coincide with the formation of knock-on electrons and x-rays, which contributes to the departure from microscopic reality. Furthermore, the application of variance reduction methods in MCNP provides complexity to the simulation. While these approaches improve efficiency by biasing particle motion, they necessarily modify the natural random movement of particle interactions. Despite these differences, when suitable weighting factors are applied, the resulting macroscopic tally produces reliable outcomes that match the results of experiments.

The pulse-height tally in MCNP differs significantly from conventional tallying methodologies used in the software. The pulse-height function operates on a different concept compared to other tallies which primarily calculate macroscopic variables such as flux by collecting large numbers of microscopic incidents. It precisely captures the energy deposited within a cell by each source and the following subsequent particles. In brief, conventional counts emphasise the precise computation of expected values for macroscopic variables, frequently missing the complexities of particular microscopic occurrences, whereas the pulse-height tally requires a more granular approach. In this approach, microscopic incident simulation requires a greater level of realism to assure data integrity.

In particle transport simulations, the pulse-height tally is a useful tool for analysing particle deposition. However, its effectiveness is limited for neutron cases due to the intrinsic non-analogue behaviour of neutron contacts. As a result, the pulse-height tally is most beneficial when counting photons and electrons, as specified by the F8 card. In photon-related issues, the F8 tally stands out as an especially effective

instrument for collecting valuable information. However, the precision of results in electron-centric models is heavily reliant on the thickness of the tallied cells. Ensuring that these cells are adequately thick is necessary for reducing mistakes caused by changes in the energy loss rate. Integrating F8 cards with photonuclear cases may be a significant issue that leads to erroneous results. While it attempts to identify incidents in the model that may affect the integrity of results, it is not perfect at recognising all such cases. As a result, it is necessary to carefully evaluate their simulation settings to ensure the requirements.

Scoring the F8 cards is an essential step at the completion of each simulation history. In circumstances without variance reduction tools, the scoring procedure becomes relatively simple and favourable for reliable data collecting. The calculation of the total deposition of energy ( $T$ ) is given in Eq. (2.5):

$$T = \sum_{i=1}^K E_i - \sum_{j=1}^L D_j \quad (2.5)$$

Where  $K$  and  $L$  denotes the number of entries and departures of specific cells, respectively. Meanwhile,  $E_i$  and  $D_j$  denotes the tally energy of  $i^{th}$  and  $j^{th}$  of particles entering and departing specific cells, respectively.

Incorporating variance reduction presents complexity to the scoring process. The F8 tally is particularly useful in simulations intended to convey the energy distribution of radiation-induced pulses within a detector. Unlike typical tallies, the F8 tally produces a total tally rather than an average, indicating the cumulative influence of scored events. While using the F8 tally, the integration of energy bin, user, and cell cards is permitted according to standards. However, the use of flagging and multiplier is restricted. In addition, the availability of cosine, time, and segment bins is subject to specific restrictions depending on the FT alternatives applied. Furthermore,

the application of dosage function (DF) and dose energy (DE) cards conflicts with the F8 tally.

Unlike other tallies, which calculate photon energy during the scoring time, the F8 tally counts the number of pulses that deposit energy inside specific bins. In brief, the energy bins in a pulse-height tally represent the energy depositions within a cell by all of the related tracks during a simulation history. Certain energy bins, such as epsilon and zero, should be specified. The inclusion of a zero bin allows for situations in which no energy deposition takes place and provides a baseline for the study. Similarly, the epsilon bin, defined by a minute energy interval, captures minor energy depositions that would have otherwise gone undetected (Werner, 2017).

## **2.6 Gaussian Energy Broadening (GEB)**

Gaussian Energy Broadening (GEB) refers to the process in which the energy distribution of detector responses generated by interactions among particles inside the detector broadens. This phenomenon occurs caused of a variety of variables, including fluctuations in the scintillation light production process, optical dispersion inside the scintillator material, and electronic noise in the detection system.

As the incident photon reaches along the path, it has several collisions and loses a portion of energy in the interaction. Nevertheless, neither the number of impacts nor the amounts of energy dissipated for each impact remain constant, leading to a dispersion of energy known as energy straggling. When calculating the overall energy of a particle with charge, energy straggling becomes insignificant. It possesses an important role during transmission investigations, in which the particle leaves the detector having only deposited a part of the energy.

Using a classical model, the distribution of the energy straggling variance is calculated as follows:

$$\sigma_E^2 = 4\pi r_0^2 (mc^2)^2 Z_1^2 Z_2 N \Delta x \quad (2.6)$$

In Eq. (2.6),  $Z_{1,2}$  denotes the charge of the incoming particle,  $Z$  is the stopping respective substance atomic number,  $D_x$  is the thickness of the material,  $N$  represents the number of atoms per  $1 \text{ m}^3$ , and  $r_0$  is particle radius.

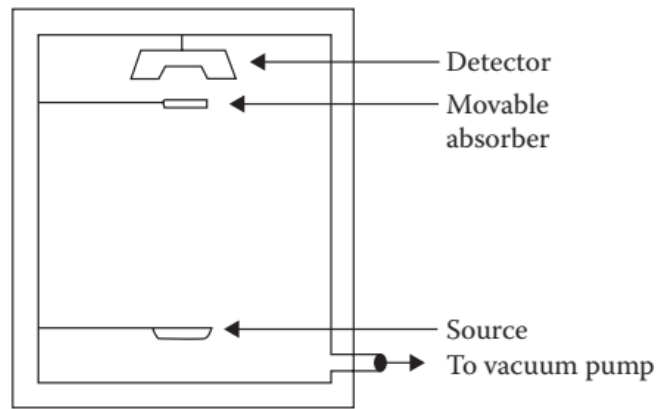


Figure 2.7 The experimental setting utilised to investigate energy straggling (Knoll, 2010)

Figure 2.7 illustrates a schematic of the experimental environment used for estimating energy straggling. An evacuated chamber houses a particle source, a detector material, and a moveable absorber, preventing energy from being lost as particles move between the source and detector. To measure the width  $\Gamma_d$ , the record of the particle energy spectrum without the absorber is conducted. The width  $\Gamma$  is determined by measuring the spectrum after placing the absorber. Eq. (2.7) is used to measure the straggling width.

$$\Gamma_s = \sqrt{\Gamma^2 - \Gamma_d^2} \quad (2.7)$$

Through the use of absorbers with various thicknesses, the dimension  $\Gamma$ 's might be examined according to its path ( $\Delta x$ ). Some studies have conducted measurements similar to this goal, particularly with alpha particles. For insignificant thicknesses, the findings from experiments are consistent with the concept, while for larger thicknesses, the theory fails to recognise the width. Figure 2.8 displays the findings for silver films with various thicknesses.

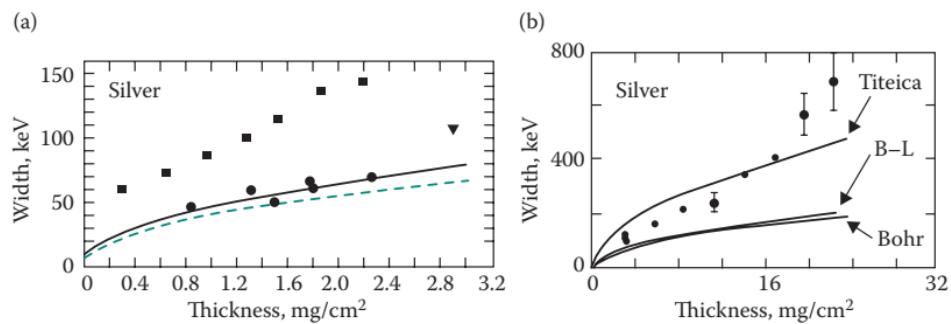


Figure 2.8 Particle straggling around A. 3.2 mg/cm<sup>2</sup> and B. 32 mg/cm<sup>2</sup> silver films (Tsoulfanidis & Landsberger, 2015)

The additional cause of GEB is the intrinsic scintillation stochasticity, which causes the emission of light photons in response to particle interactions to vary statistically. Moreover, optical errors and impurities in the scintillator material could lead to the widening of the energy distribution. Furthermore, electronic noise occurring through the signal readings process could increase the influence of GEB, broadening the detector's energy response.

The broadening of the energy distribution caused by GEB exhibits a major impact on detector performance. This might result in lower energy resolution, limiting the detector's capacity to precisely identify and measure the energies of incoming particles. As a result, appropriate correction procedures are required to limit the effects

of GEB and assure the accuracy of radiation observations acquired using scintillation detectors.

A variety of adjustment approaches have been implemented to overcome GEB and increase the resolution of detectors. These approaches frequently include mathematical modelling of the energy distribution, which is then followed by the use of filters or deconvolution methods to improve resolution. It is expected to efficiently reduce the influence of GEB and optimise the performance of detectors for a variety of radiation detection and measurement applications by adopting adequate correction procedures. Understanding the fundamental origins and consequences of GEB is critical for appropriately interpreting experimental results and optimising detector performance. The negative impacts of GEB can be minimised by developing and using sophisticated correction procedures, resulting in increased energy resolution and radiation measurement reliability.